

WATER EVAPORATION FROM POROUS MEDIA

Lorne A. Davis, Jr.

Department of Physics, Texas Lutheran University, USA

This paper was prepared for presentation at the International Symposium of the Society of Core Analysts held in Austin, Texas, USA 18-21 September, 2011

ABSTRACT

Drying is one of the fundamental unit operations in manufacturing, agriculture, and food production. Interestingly, evaporation of water from a porous material can be faster than from the bulk liquid. Motivation for this work arises from the manufacturing of porous materials and the engineering use of matrix-assisted transport. A special core analysis technique, low-field nuclear magnetic resonance (NMR) relaxometry, observed water drying from consolidated and unconsolidated porous samples. The amplitude response provided water content and drying rate, and the T_2 relaxation distributions provided the water pore distribution during drying and insight into the internal transport mechanism.

In accord with current drying models, three major drying regimes were evident. An early constant rate period (CRP) declined linearly with water saturation S_w . Subsequently, the first falling rate period (FRP1) ultimately declined as the square root of time. Following this, for $S_w < S_{w,ir}$, the irreducible water saturation, a second falling rate period (FRP2) had an even slower square-root drying dependence. Measurements of sample-averaged T_2 distributions support the concept of capillarity-driven thinning-film pore water transport in CRP mode and stochastic, discontinuous transport of pore-filling blobs in FRP mode.

The relation of drying to sample geometry, pore size, and pore structure was determined using seven consolidated porous media and three unconsolidated samples (silica sand, kaolinite clay, and montmorillonite clay). Due to a fast ^1H exchange rate, accurate NMR total water measurement was possible for the swelling montmorillonite, which had significant interlamellar water. In addition, the montmorillonite interlamellar-interstitial mass transfer step did not slow its drying rate compared to the kaolinite clay rate. The sand dried in CRP mode until $S_{w,ir}$, but both clay rates lessened for $S_w < 0.5$. However, the T_2 -evidenced pore water transport mechanism in the clays appeared to stay in CRP mode.

THEORY

Early drying models, e.g. by Washburn, were diffusion analogs with limited predictive range and validity. [1] Recent theories using either a coupled-field mass-energy transport model or a pore network percolation model agree in their general description of the various drying regimes. [2, 3] As depicted in Figure 1, the drying in the constant rate period (CRP) is approximately linear with time; capillary rise has the rate capability to deliver sufficient water flux to maintain a uniform water surface film until hydraulic continuity is broken. MRI profile imaging has confirmed uniform internal water

saturation during CRP drying. [4] The first falling rate period (FRP1) ensues when a percolation threshold is reached, and the surface water breaks into patches. In the second falling rate period (FRP2), the surface is dry, a drying front propagates backward, and the drying proceeds even more slowly, at the rate of tortuous unsaturated vapor diffusion.

EXPERIMENTAL METHODOLOGY

An Oxford Instruments Maran Ultra DRX2 2MHz NMR collected T_2 relaxation data every half hour using a CPMG pulse sequence with a $100\mu\text{s}$ pulse gap (τ). The sample was at 33C under no confining stress and centered in an open topped glass cylinder, allowing for natural convection. Room humidity stayed $\sim 50\%$. The T_2 multi-exponential distributions were derived using singular value decomposition (SVD) in *Medusa*, a GUI-based routine written locally in MATLABTM. Data signal-to-noise determined the default number of singular values. The outputs were the total NMR amplitude (water content) and the T_2 distribution used in mapping the pore characteristics of soil and rock. [5]

The sand (average grain size $\sim 115\mu$), Na-montmorillonite clay (Bentonite), and kaolinite clay (Kaolin) were from Ward's Natural Science, identified as #45W1983, #46E0435, and #46E0995, respectively. These materials, characterized in Table 1, were further sorted, packed under vibration to the same final length in TeflonTM vials in small aliquots of alternating dry grains and distilled water, and aged at least three months. The free top surface accommodated the necessary expansion of the Bentonite. The Bentheim sandstone from Temco, Inc., the alumina from Refractron Technologies, Corp., and the fired clay plugs from Soilmoisture Equipment Corp are characterized in Table 2. Mercury porosimetry provided average pore throat diameters. After distilled water saturation and aging, they were wrapped in SaranTM with only the top face exposed for the drying. In both tables the scaled pore size from NMR is given in terms of T_{2LM} , the log mean T_2 .

RESULTS AND CONCLUSIONS

For all cases examined, the porous medium drying rate was initially greater than the evaporation rate of bulk water. Figure 2 shows typical cases for S_w in consolidated media. Samples AF15, AF03, B01M1, and B03M1 of Table 1 all dry at constant flux rate, i.e. constant slope. The FRP2 mode begins near irreducible water saturation S_{wir} . As shown in figure 3, plug AF35, with a larger pore size, dried first in CRP mode, then in FRP1 mode for lower S_w values. Plug AF70, with the largest pore size, dried in FRP1 mode from the start of drying. In all observations, with both thermal and mildly forced convection, an observed FRP rate was asymptotically proportional to the square root of time (figure 3), suggestive of a diffusive mechanism and Washburn's drying equation. [1]

Figure 4 contrasts the relation between observed T_{2LM} and S_w for representative CRP and FRP1 mode drying. Using the definition of R_{T2} as the ratio of T_{2LM} @ S_w to T_{2LM} @ $S_w = 1$, in the CRP mode R_{T2} scales one-to-one with S_w , as is modeled by assuming the fast diffusion limit and a fully water-wet pore wall. Under these assumptions, the CRP mode pore drying model derives from the saturated T_2 relationship by simple extrapolation:

$$\text{Saturated: } T_2 = (V/S)/\rho_2 \rightarrow \text{Under-Saturated: } T_2 = S_w * (V/S)/\rho_2, \quad (1)$$

where the fully saturated pore volume/surface ratio is V/S and ρ_2 is the T_2 relaxivity. [6] The time evolution of the T_2 distributions for sample B01M1 (figure 5) is characteristic of all CRP mode drying and agrees with this model's prediction: $R_{T_2} = S_w$. For this CRP model, the surface drying rate is the controlling rate, capillary rise would be the film driving force, and pore airflow would be counter-current. For the FRP1 drying of AF35 and AF70 (figure 6), the relaxation ratio R_{T_2} depends only weakly on S_w , and the main T_2 peak location is static, implying blob-type water transport with decreasing total pore surface coverage. A relevant model would require pores in the main peak to drain stochastically in rheon-like jumps with little intermediate air saturations. [7] Interestingly, T_2 distribution measurements in FRP mode all contained much more noise at all S_w .

Figure 7 describes the only fan-aided forced convection referenced in this work, two identically sized Bentheim sandstone plugs epoxied either on the cylinder side or on both ends. When the drying traversal length was radial, the drying stayed in the capillarity-driven CRP mode (with constant rate and uniform S_w) until S_{wir} . For drying along the axis, the longer dimension, the drying entered FRP1 mode at $S_w \sim 0.5$. Thus, the drying mode is determined by extrinsic, as well as intrinsic, matrix properties. This seems analogous to the lumped system approximation for heat flow in a body, in which the body cools with uniform internal temperature if the dimensionless Biot number is below 0.1.

A T_2 CPMG NMR sequence with a tau of $100\mu s$ accurately measured water in the clays. As shown in Figure 8, total water content, interstitial plus interlamellar for the montmorillonite, had a linear response. Montmorillonite interlamellar pores are 0.96-2.14 nm, much smaller than interstitial pores. [8] Non-exchanging interlamellar pores should have a T_2 peak much smaller than the interstitial peak, or be unobservable, depending on the relaxivity. [6] However, as observed here and elsewhere, there is one intermediately positioned peak, indicating that interlamellar water is in fast spin exchange with interstitial water. [9, 10] Thus the spin information for this clay is exchanged on a time scale less than the NMR experiment (\sim tau), and the NMR technique is appropriate. [9]

The interlamellar-interstitial diffusional mass transport was not a retarding factor in the Bentonite drying. This rate has been estimated to be about an hour, fast compared to the drying. [6] As seen in Figure 9, the early mass flux drying rates of both clays and the sand are the same, as expected for CRP mode drying. Their linear R_{T_2} - S_w relations (figure 10) determine that the drying of all three remain in the CRP film transport mode until S_{wir} , even though both clays exhibit the same atypical rate decline below $S_w \sim 0.5$.

ACKNOWLEDGEMENTS

The author gratefully acknowledges a grant from the W. M. Keck Foundation to establish an undergraduate education program in transport phenomena. Summer research students Lauren Alexander, Caleb Bahr, Dylan Ginn, Kelsey Hallford, Dielli Hoxha, Ryan

Patterson, Aaron Rea, Aaron Sansom, and Jessica White contributed to software development, procedure development, and/or sample preparation. Dirk Lorenz (now a graduate student in physics at Rice University) wrote the *Medusa* SVD computational engine, and Curtis Lee (now a graduate student in civil engineering at Duke University) extended the software to bulk processing. The author thanks Dr. Chris Christenson of Dow Chemical Co. for encouragement and supporting information.

REFERENCES

1. Washburn, E. W., "The Dynamics of Capillary Flow", *Physical Review*, (1921) **17**, 3, 273-283.
2. Zhang, Z., Yang, S., and Liu, D., "Mechanism and Mathematical Model of Heat and Mass Transfer During Convective Drying of Porous Materials", *Heat Transfer — Asian Research*, (1999) **28**, 5, 337-351.
3. Yiotis, A. G., Tsimpanogiannis, I. N., Stubos, A. K., Yortos, Y. C., "Pore-Network Study of the Characteristic Periods in the Drying of Porous Materials", *Journal of Colloid and Interface Science*, (2006) **297**, 738-748.
4. Peysson, Y., Fleury, M., Norrant, F., and Pascual, V. B., "Diffusive and Convective Drying on a Shaly Sandstone Using NMR Measurements", Paper 2009-34 presented at the International Symposium of the Society of Core Analysts held in Noordwijk, The Netherlands 27-30 September 2009.
5. Bayer, J. V., Jaeger, F., and Schaumann, G. E., "Proton Nuclear Magnetic Resonance (NMR) Relaxometry in Soil Science", *The Open Magnetic Resonance Journal*, (2010) **3**, 15-26.
6. Kleinberg, R. L., "Utility of NMR T_2 Distributions, Connection with Capillary Pressure, Clay Effect, and Determination of the Surface Relaxivity Parameter ρ_2 ", *Magnetic Resonance Imaging*, (1996) **14**, 7/8, 761-767.
7. Dullien, F.A., *Porous Media Fluid Transport and Pore Structure*, 2nd Ed., Academic Press, New York, 1992, 163-165.
8. Tucker, M. E., *Sedimentary Petrology*, Blackwell Scientific, Boston, 1985, 81-84.
9. Woessner, D. E. and Snowden, B. S., Jr., "A Study of the Orientation of Adsorbed Water Molecules on Montmorillonite Clays by Pulsed NMR", *Journal of Colloid and Interface Science*, (1969) **30**, 1, 54-68.
10. Hum, F. and Kantzas, A., "Using Low Field NMR to Understand Fines Behaviour", Paper 2005-46 presented at the International Symposium of the Society of Core Analysts held in Toronto, Canada 21-25 August 2005.

TABLES AND FIGURES

Table 1. Characterization of Unconsolidated Sand and Clay Plugs

Porous Matrix	Face Area, A (cm ²)	Length, L (cm)	Initial Water Mass, M (g)	Dry Matrix Mass (g)	T _{2LM} * (ms)
Silica sand	5.07	~3.5	5.38	29.96	180
Kaolin	5.07	~3.5	10.44	15.04	13.7
Bentonite	5.07	~3.6	18.18	5.92	12.1

Table 2. Characterization of Consolidated Plugs

Porous Matrix	Face Area, A (cm ²)	Length, L (cm)	Porosity, ϕ (cm ³ /cm ³)	Pore Throat Diameter (μ m)	T _{2LM} * (ms)
Bentheim SS	4.58	5.04	---	---	450
Alumina AF70	5.32	4.06	0.298	94.6	970
Alumina AF35	5.36	3.96	0.433	31.9	728
Alumina AF15	5.28	4.10	0.407	21.3	618
Alumina AF03	4.38	3.53	0.547	4.14	224
Fired Clay B01M1	5.08	2.59	0.341	0.500	53.4
Fired Clay B03M1	5.08	2.55	0.381	0.221	6.55

* T_{2LM} as measured at S_w = 1. The T₂ of the bulk distilled water was 2.95 s.

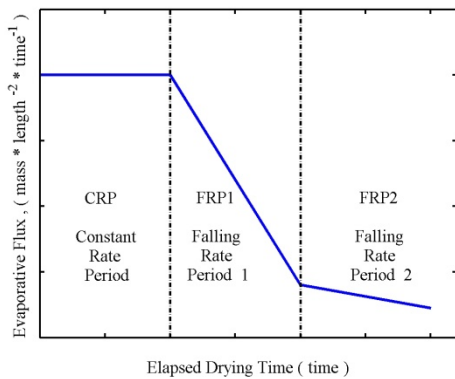


Figure 1. Idealized Model of Drying History of a Porous Medium

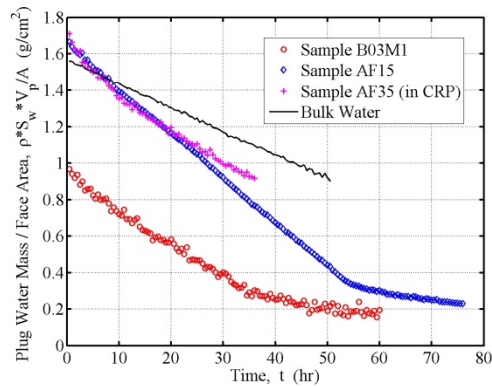


Figure 2. CRP Drying: Consolidated Sample Rate Histories

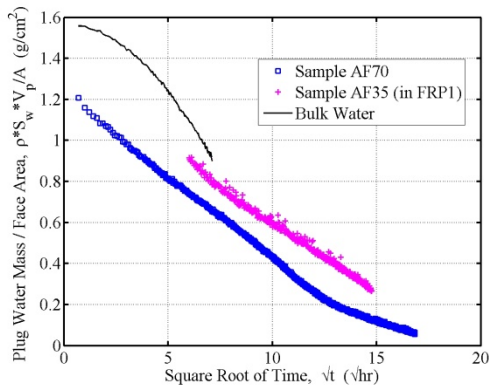


Figure 3. FRP1 Drying: Consolidated Sample Rate Histories

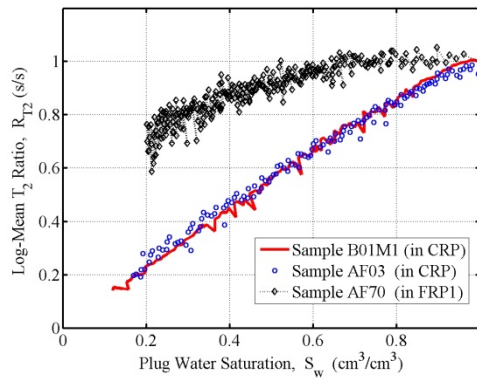


Figure 4. CRP and FRP1 Drying: Consolidated Sample Scaled T_{2LM} Histories

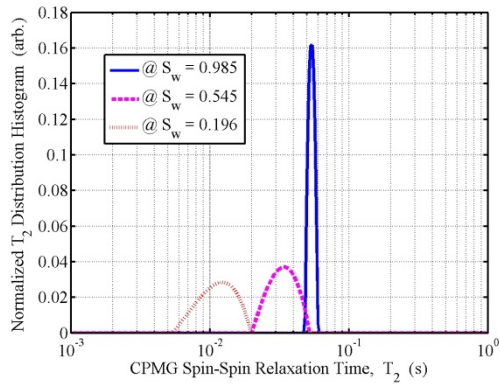


Figure 5. CRP Drying: Sample B01M1 Normalized T_2 Distributions

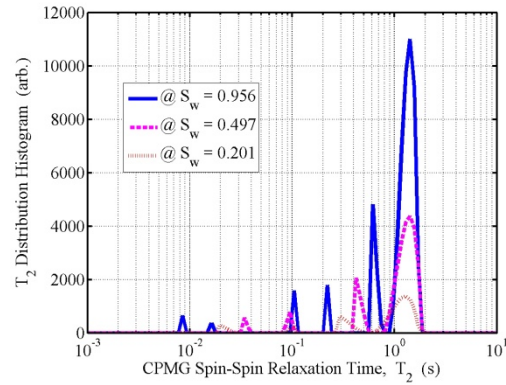


Figure 6. FRP1 Drying: Sample AF70 Non-Normalized T_2 Distributions

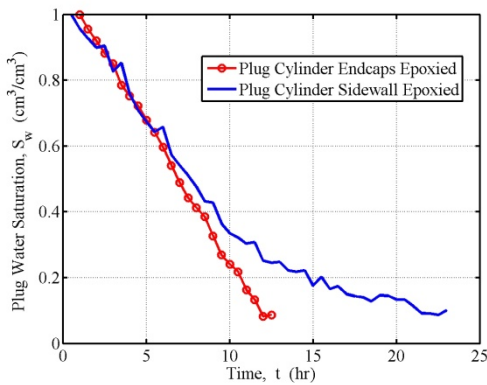


Figure 7. Bentheim SS Drying as a Function of Face Geometry

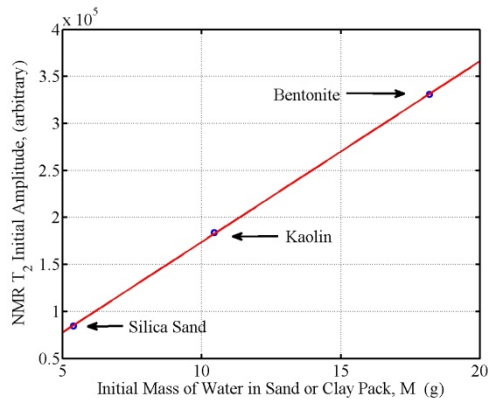


Figure 8. NMR CPMG Water Calibration for Saturated Sand and Clays

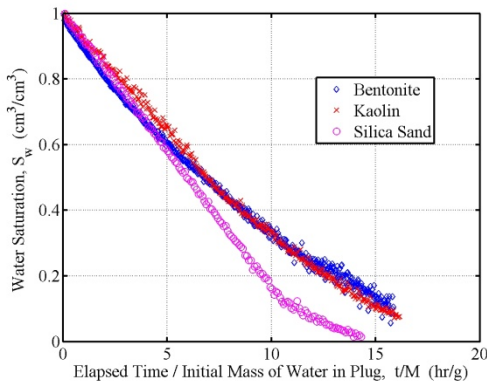


Figure 9. CRP and FRP1 Drying: Scaled Rate Histories for Sand and Clay Packs

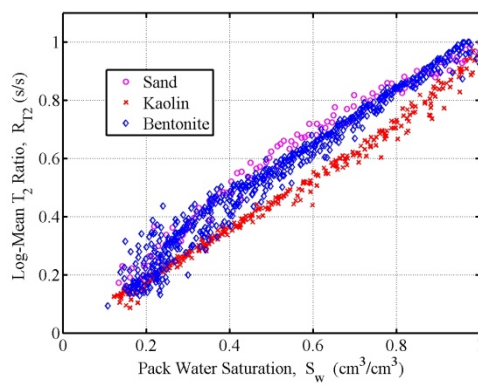


Figure 10. CRP and FRP1 Drying: Scaled T_{2LM} Histories for Sand and Clay Packs